

Engineering

Industrial & Management Engineering fields

Okayama University

Year 1995

Shape from shading with interreflections
under proximal light source - 3D shape
reconstruction of unfolded book surface
from a scanner image

Toshikazu Wada
Okayama University

Hiroyuki Ukida
Okayama University

Takashi Matsuyama
Okayama University

This paper is posted at eScholarship@OUDIR : Okayama University Digital Information Repository.

<http://escholarship.lib.okayama-u.ac.jp/industrial-engineering/58>

Shape from Shading with Interreflections under Proximal Light Source

— 3D shape Reconstruction of Unfolded Book Surface from a Scanner Image —

Toshikazu WADA

Hiroyuki UKIDA

Takashi MATSUYAMA

Department of Information Technology, Faculty of Engineering,
OKAYAMA UNIVERSITY

3-1-1, Tsushima Naka, Okayama-shi, Okayama 700, JAPAN

Abstract

In this paper, we address the problem to recover the 3D shape of an unfolded book surface from the shading information in a scanner image. From a technical point of view, this shape from shading problem in real world environments is characterized by 1) proximal light source, 2) interreflections, 3) moving light source, 4) specular reflection, and 5) nonuniform albedo distribution. Taking all these factors into account, we first formulate the problem based on an iterative non-linear optimization scheme. Then we introduce piecewise polynomial models of the 3D shape and albedo distribution to realize efficient and stable computation. Finally we propose a method of restoring the distorted scanner image based on the reconstructed 3D shape. Image restoration experiments for real book surface demonstrated that geometric and photometric distortions are almost completely removed by the proposed method.

1 Introduction

In this paper, we address the problem to recover the 3D shape of an unfolded book surface from the shading information in a scanner image. From a technical point of view, this shape from shading problem in real world environments is characterized by the following properties:

1. *Proximal light source:* The light source of an image scanner is located very close to the book surface. This implies that the illuminant intensity and the light source direction vary with locations on the book surface.
2. *Interreflections:* The light reflected on one side of an unfolded book surface illuminates the other.
3. *Moving light source:* The light source moves during the scanning process.
4. *Specular reflection:* The book surface is not Lambertian.
5. *Nonuniform albedo distribution:* The albedo distribution over a book surface is not uniform.

In the following sections, we first formulate this real world shape from shading problem based on an iterative non-linear optimization scheme. Then we introduce piecewise polynomial models of the 3D shape and albedo distribution to realize efficient and stable computation. In the last part of the paper, we propose a method of restoring the distorted scanner image based on the reconstructed 3D shape and demonstrate the effectiveness and efficiency of the proposed methods with several experiments using scanner images of real books.

2 Problem Formulation

First, we consider the *ideal* shape from shading problem under the following conditions:

- a. The light source is distant from the object surface. This implies that the illuminant intensity and the light source direction are constant all over the object surface.
- b. There are no interreflections.
- c. The location of the light source is fixed.
- d. The object surface is Lambertian.
- e. The albedo is constant all over the object surface.

The problem under these ideal conditions is formulated as:

$$I_o(\mathbf{x}) = \rho \cdot I_s \cdot \cos \varphi(\mathbf{x}), \quad (1)$$

where \mathbf{x} denotes a 2D point in the image, $I_o(\mathbf{x})$ the reflected light intensity observed at \mathbf{x} , I_s the illuminant intensity, ρ the albedo on the surface, and $\varphi(\mathbf{x})$ the angle between the light source direction and the surface normal at the 3D point on the object surface corresponding to \mathbf{x} .

In this case, $\varphi(\mathbf{x})$ can easily be calculated when $\rho \cdot I_s$ is given¹. Then, the shape of the object surface can be computed from $\varphi(\mathbf{x})$ by introducing some additional constraints: photometric stereo[2]

¹For example, we can determine $\rho \cdot I_s$ assuming that $\varphi(\mathbf{x})$ is equal to zero at \mathbf{x} where $I_o(\mathbf{x})$ takes the maximum value.

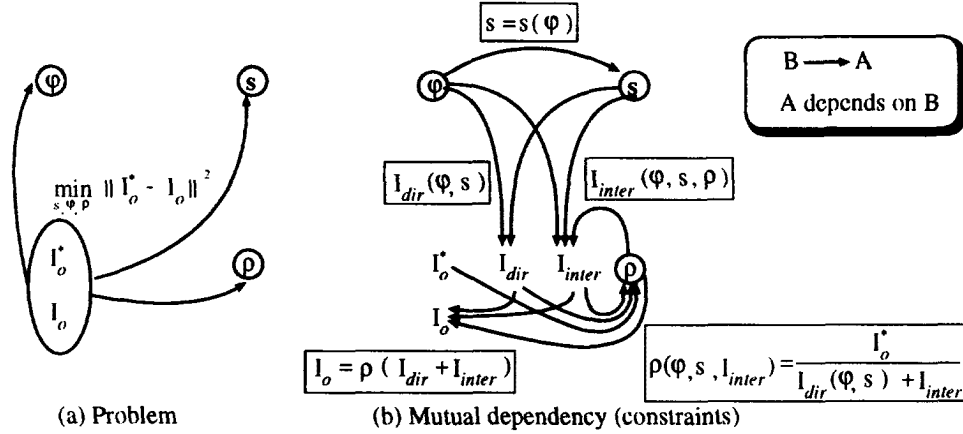


Figure 1: Structure of the problem

and shape constraints such as smoothness[3] and cylindrical surface[4].

Next, we describe a stepwise formulation of our shape from shading problem under characteristics 1~5 described before.

Proximal light source(characteristic 1.)

$$I_o(\mathbf{x}) = \rho \cdot I_s(d(\mathbf{s}(\mathbf{x}), \mathbf{l})) \cdot \cos \varphi(\mathbf{x}), \quad (2)$$

where \mathbf{l} denotes the 3D location of the light source, $\mathbf{s}(\mathbf{x})$ the 3D point on the object surface corresponding to \mathbf{x} , and $d(\mathbf{s}(\mathbf{x}), \mathbf{l})$ the distance between \mathbf{l} and $\mathbf{s}(\mathbf{x})$. We assume that ρ and \mathbf{l} are given. Note that in this problem, the absolute location (depth) of the object surface $\mathbf{s}(\mathbf{x})$ is required to compute $\varphi(\mathbf{x})$.

Interreflections[5](characteristic 2.)

$$I_o(\mathbf{x}) = \rho \left\{ I_s + \int \frac{I_o(\mathbf{x}')}{\{d(\mathbf{s}(\mathbf{x}), \mathbf{s}(\mathbf{x}'))\}^2} d\mathbf{x}' \right\} \cos \varphi(\mathbf{x}). \quad (3)$$

In this formulation, we assume that 1) the light reflected at $\mathbf{s}(\mathbf{x}')$ can reach $\mathbf{s}(\mathbf{x})$ for any \mathbf{x} and \mathbf{x}' , 2) the light reflected more than once is enough attenuated to be neglected. Note that with interreflections, the global shape of the object surface ($\forall \mathbf{x}' d(\mathbf{s}(\mathbf{x}), \mathbf{s}(\mathbf{x}'))$) is required to compute $\varphi(\mathbf{x})$.

Interreflections under proximal light source (characteristics 1 and 2)

$$I_o(\mathbf{x}) = \rho \left\{ I_s(d(\mathbf{s}(\mathbf{x}), \mathbf{l})) + \int \frac{I_o(\mathbf{x}')}{\{d(\mathbf{s}(\mathbf{x}), \mathbf{s}(\mathbf{x}'))\}^2} d\mathbf{x}' \right\} \times \cos \varphi(\mathbf{x}). \quad (4)$$

In this case, the overall depth ($\forall \mathbf{x} \mathbf{s}(\mathbf{x})$) of the object surface is required to compute $\varphi(\mathbf{x})$.

Under moving light source(characteristics 1~3)

$$I_o(\mathbf{x}) = \rho \left\{ I_s(d(\mathbf{s}(\mathbf{x}), \mathbf{l}(\mathbf{x}))) + \int \frac{I_o(\mathbf{x}')}{\{d(\mathbf{s}(\mathbf{x}), \mathbf{s}(\mathbf{x}'))\}^2} d\mathbf{x}' \right\} \times \cos \varphi(\mathbf{x}), \quad (5)$$

where $I_o'(\mathbf{s}(\mathbf{x}'), \mathbf{l}(\mathbf{x})) = \rho \cdot I_s(d(\mathbf{s}(\mathbf{x}'), \mathbf{l}(\mathbf{x}))) \cdot \cos \varphi(\mathbf{x}')$ and $\mathbf{l}(\mathbf{x})$ denotes the light source location corresponding to \mathbf{x} , which we assume is given a priori. Under a moving light source, $I_o'(\mathbf{s}(\mathbf{x}'), \mathbf{l}(\mathbf{x}))$ must be calculated at each point on the object surface. Hence, the computation becomes more expensive than that under a fixed light source[5].

The addressed problem(characteristics 1~5)

$$I_o(\mathbf{x}) = \left\{ I_s(d(\mathbf{s}(\mathbf{x}), \mathbf{l}(\mathbf{x}))) + \int \frac{I_o'(\mathbf{s}(\mathbf{x}'), \mathbf{l}(\mathbf{x}))}{\{d(\mathbf{s}(\mathbf{x}), \mathbf{s}(\mathbf{x}'))\}^2} d\mathbf{x}' \right\} \times \rho(\mathbf{s}(\mathbf{x})) \times f(\varphi(\mathbf{x}), \mathbf{s}(\mathbf{x})), \quad (6)$$

where $I_o'(\mathbf{s}(\mathbf{x}'), \mathbf{l}(\mathbf{x})) = \rho(\mathbf{s}(\mathbf{x}')) \cdot I_s(d(\mathbf{s}(\mathbf{x}'), \mathbf{l}(\mathbf{x}))) \cdot f(\varphi(\mathbf{x}'), \mathbf{s}(\mathbf{x}'))$, $\rho(\mathbf{s}(\mathbf{x}))$ denotes the albedo and $f(\varphi(\mathbf{x}), \mathbf{s}(\mathbf{x}))$ the reflectance property at point $\mathbf{s}(\mathbf{x})$. In this problem, $\forall \mathbf{x} \mathbf{s}(\mathbf{x})$ and $\forall \mathbf{x} \rho(\mathbf{s}(\mathbf{x}))$ are required to compute $\varphi(\mathbf{x})$.

3 Solution Scheme

Equation (6) can be rewritten as:

$$I_o(\mathbf{s}, \varphi, \rho) = \rho \times (I_{dir}(\mathbf{s}, \varphi) + I_{inter}(\mathbf{s}, \varphi, \rho)), \quad (7)$$

where

$$I_{dir}(\mathbf{s}, \varphi) = f(\varphi(\mathbf{x}), \mathbf{s}(\mathbf{x})) \times I_s(d(\mathbf{s}(\mathbf{x}), \mathbf{l}(\mathbf{x}))) \quad (8)$$

$$I_{inter}(\mathbf{s}, \varphi, \rho) = f(\varphi(\mathbf{x}), \mathbf{s}(\mathbf{x})) \times \int \frac{I_o'(\mathbf{s}(\mathbf{x}'), \mathbf{l}(\mathbf{x}))}{\{d(\mathbf{s}(\mathbf{x}), \mathbf{s}(\mathbf{x}'))\}^2} d\mathbf{x}'. \quad (9)$$

Using these notations, we discuss why and how this problem can be solved.

3.1 Why can the problem be solved ?

Based on the optimization scheme, the problem can be formulated as that of finding \mathbf{s} , φ and ρ which minimize the following objective functional (Figure 1 (a)):

$$\begin{aligned} F(\mathbf{s}, \varphi, \rho) &= \|I_o(\mathbf{s}, \varphi, \rho) - I_o^*\|^2 \\ &= \|\rho \times (I_{dir}(\mathbf{s}, \varphi) + I_{inter}(\mathbf{s}, \varphi, \rho)) - I_o^*\|^2 \end{aligned} \quad (10)$$

where I_o^* represents the observed intensity.

If all the argument functions of F are independent of each other, this problem can be solved numerically by some optimization algorithm. In our case, however, the argument functions s , φ and ρ have such mutual dependencies as described below (Figure 1 (b)):

- If the object has a smooth surface, s and φ depend on each other. Here we assume that 1) the depth of a point on the object surface is known and 2) the object surface is smooth. Under these assumptions, s can be represented as:

$$s = s(\varphi). \quad (11)$$

- At the end of the optimization process, $I_o(s, \varphi, \rho)$ should be approximately equal to the observed intensity I_o^* . Hence, $I_o(s, \varphi, \rho)$ in equation (7) can be substituted by I_o^* , and we obtain the following equation ²:

$$\rho = \frac{I_o^*}{I_{dir}(s, \varphi) + I_{inter}(s, \varphi, \rho)}. \quad (12)$$

Because of these complicated mutual dependencies among the argument functions, our problem seems to be hardly solved. But, the mutual dependency can be unraveled as follows:

1. From equation (11), s can be computed from φ .
2. From equation (12), it is obvious that the value ρ essentially depends on s and φ .
3. From 1 and 2, both s and ρ essentially depend on φ . Consequently, the only independent argument of the objective functional F is φ .

In short, our problem is essentially equivalent to an ordinary optimization problem of a functional F with a single argument function φ . Hence, the problem can essentially be solved.

3.2 How to solve the problem?

As discussed above, the problem is equivalent to an ordinary optimization problem. In practice, however, the problem can not be solved by ordinary optimization algorithms, because the value of the objective functional F can not be directly computed from φ . The essential difficulty is that I_{inter} in equation (9) and ρ in equation (12) mutually depend on each other and the mutual dependency cannot be solved algebraically, which lead us to the numerical solution.

For the numerical computation of ρ and I_{inter} , we decompose equation (12) to the following two equations:

$$I_{inter} = I_{inter}(s, \varphi, \rho), \quad (13)$$

$$\rho = \rho(s, \varphi, I_{inter}) = \frac{I_o^*}{I_{dir}(s, \varphi) + I_{inter}}. \quad (14)$$

By computing I_{inter} and ρ iteratively by the above equations³ for fixed values s and φ , ρ and I_{inter} will converge to proper values. This iteration is considered as a procedure to compute $I_{inter}(s, \varphi)$ and $\rho(s, \varphi)$.

²Unfortunately, the algebraic representation of ρ can not be obtained from equation (12), because both sides of this equation include ρ .

³ $I_{inter}(s, \varphi, \rho)$ is computed from equation (9).

By embedding the optimization procedure for $\min_{s, \varphi} F$ into the above iterative procedure, we obtain the following algorithm to solve the problem:

Initial estimate: By neglecting the term I_{inter} , compute initial estimation of s , φ and ρ .

Step 1: Compute I_{inter} from the estimated s , φ and ρ .

Step 2: Compute s and φ which minimize the objective functional F for fixed I_{inter} and ρ .

Step 3: Compute ρ from the estimated s , φ and I_{inter} .

If the objective functional exceeds the given threshold then goto **Step 1**.

The detailed algorithm is described later.

4 Practical Model

4.1 Geometric Models

Figure 2 shows the structure of the image scanner and the coordinate system to describe the problem. The sensor D takes a 1D image $P^*(x_i)$ along the scanning line S and moves with L , M and C . The sequence of $P^*(x_i)$ s forms a 2D image $P^*(x_i, y_j)$. Note that while $P^*(x_i)$ is obtained by the perspective projection, the projection along the y -axis is equivalent to the orthogonal projection.

We introduce the following assumptions about the geometric configuration of the book surface:

- (1) The book surface is cylindrical and the shape of its cross section on the $y-z$ plane is smooth except for the point separating book pages.
- (2) The unfolded book surface is aligned on the scanning plane so that the center line separating book pages is just above the x -axis.

These assumptions reduce the 3D shape reconstruction problem to the 2D cross section shape reconstruction problem. That is, φ and s is reduced to 1D functions of y .

4.2 Optical Model

The relationship between the image intensity and the reflected light intensity is formulated as follows:

$$P(x_i, y_j) = \alpha \cdot \rho(x_i, y_j) (I_{dir}(x_i, y_j) + I_{inter}(x_i, y_j)) + \beta, \quad (15)$$

where

- $P(x_i, y_j)$: The image intensity at (x_i, y_j) in the observed image.
- α, β : Parameters of the photoelectric transformation in the image scanner.
- $I_{dir}(x_i, y_j)$: The reflected light component corresponding to the direct illumination from the light source.
- $I_{inter}(x_i, y_j)$: The reflected light component corresponding to the indirect illumination from the opposite side of the book surface.

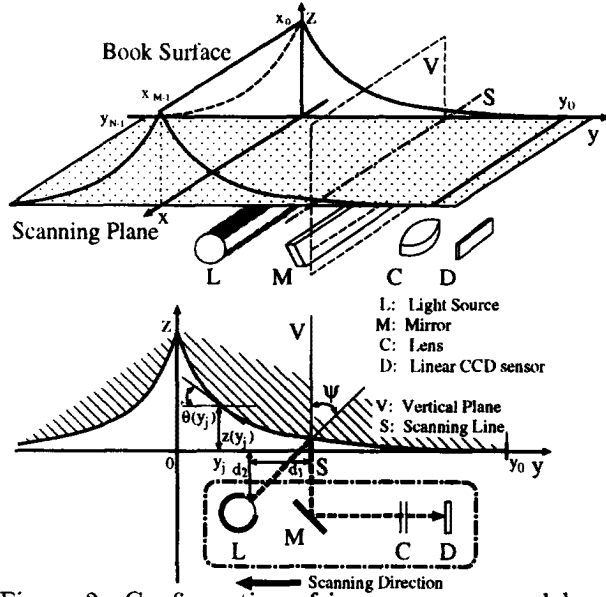


Figure 2: Configuration of image scanner and book surface

$I_{dir}(x_i, y_j)$ and $I_{inter}(x_i, y_j)$ are formulated as follows:

$$I_{dir}(x_i, y_j) = I_s(y_j, z(y_j), y_j) \cdot f(\mathbf{n}_1, \mathbf{l}_1, \mathbf{v}_1), \quad (16)$$

$$I_{inter}(x_i, y_j) = A \sum_{y_n=y_0}^{y_{N-1}} V(y_n, y_j) \cdot I_s(y_n, z(y_n), y_j) \times \sum_{x_m=x_0}^{x_{M-1}} \rho(x_m, y_n) \frac{f(\mathbf{n}_2, \mathbf{l}_2, \mathbf{v}_2) \cdot f(\mathbf{n}_1, \mathbf{l}_3, \mathbf{v}_1)}{\{d(x_m, y_n, x_i, y_j)\}^2}, \quad (17)$$

where

• $z(y_j)$: The distance between the scanning plane and the book surface (see Figure 2). That is, $z(y_j)$ is the practical representation of s . $z(y_j)$ is represented as follows:

$$z(y_j) = \sum_{y_k=y_0}^{y_j} \tan \theta(y_k) \quad (0 < y_j < y_0), \quad (18)$$

where $\theta(y_j)$ is the slant angle of the surface. That is, $\theta(y_j)$ is the practical representation of φ and equation (18) corresponds to $s(\varphi)$ in equation (11).

• $I_s(y, z, y_j)$: The illuminant intensity distribution on the y - z plane when taking the 1D image at y_j . Using the linear light source model, $I_s(y, z, y_j)$ is formulated as follows:

$$I_s(y, z, y_j) = \frac{I_D(\psi(y, z, y_j))}{\sqrt{(y - (y_j - d_1))^2 + (z + d_2)^2}} + I_e, \quad (19)$$

$$\psi(y, z, y_j) = \arctan \left(\frac{y - (y_j - d_1)}{z + d_2} \right), \quad (20)$$

where $(y_j - d_1, -d_2)$ denotes the location of the light source on the y - z plane, $\psi(y, z, y_j)$ the angle between

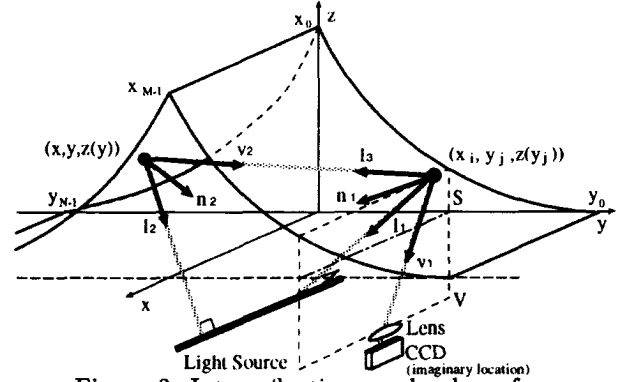


Figure 3: Interreflections on book surface

the vertical line and the light source direction, $I_D(\psi)$ the directional distribution of the illuminant intensity, and I_e the environment light intensity (see Figure 2).
• $f(\mathbf{n}, \mathbf{l}, \mathbf{v})$: The reflectance property on the book surface. We employ the Phong's model[6] to represent both the diffuse and specular components of the reflected light.

$$f(\mathbf{n}, \mathbf{l}, \mathbf{v}) = s \cos \varphi(\mathbf{n}, \mathbf{l}) + (1 - s) \cos^n \delta(\mathbf{n}, \mathbf{l}, \mathbf{v}), \quad (21)$$

where \mathbf{n} denotes the surface normal, \mathbf{l} the direction of the illumination, and \mathbf{v} the view point direction. $\mathbf{n}, \mathbf{l}, \mathbf{v}$ are corresponding to $\mathbf{n}_1, \mathbf{l}_1, \mathbf{v}_1, \dots$ etc. as shown in Figure 3. φ denotes the angle between \mathbf{n} and \mathbf{l} , and δ the angle between \mathbf{v} and the direction of the specular reflection. s, n are the parameters to specify the reflectance property.

• A : The area size of a pixel in the image.
• $V(y_n, y_j)$ (the visibility function): If the light reflected at $(x_m, y_n, z(y_n))$ can reach $(x_i, y_j, z(y_j))$, then this function takes 1. Otherwise 0.

In the experiments, parameters ($\alpha, \beta, d_1, d_2, I_e, s, n, I_D(\psi)$) are estimated a priori by using images of white flat slopes with known slants.

5 Shape Reconstruction

Under the practical conditions described in the previous section, the problem now becomes that of estimating the shape $\theta(y_j)$, the depth $z(y_j)$ and the albedo $\rho(x_i, y_j)$ which minimize the total error between the observed image intensity $P^*(x_i, y_j)$ and the image intensity model $P(x_i, y_j)$ calculated from equation (15). The depth $z(y_j)$ can be calculated from $\theta(y_j)$ by equation (18) and the albedo $\rho(x_i, y_j)$ from $\theta(y_j), z(y_j)$ and $P^*(x_i, y_j)$ by equation (15). Hence, the problem is essentially equivalent to estimating optimal $\theta(y_j)$ s which minimize the total error.

This estimation problem can be formalized as a non-linear optimization problem in N -dimensional space, where N represents the number of sampling points along the y axis. To compute the numerical solution of this problem, simultaneous equations with $N \times N$ coefficient matrix must be solved iteratively. In a practical problem, however, there are thousands of sampling points, and hence, such naive computation

becomes extremely expensive. Moreover, local noise in an image introduces errors into $\theta(y_j)$ s, which are accumulated by equation (18) and lead to global errors in $z(y_j)$ s.

5.1 Piecewise Shape and Albedo Approximation

To improve the computational efficiency and the stability, we employ the following two piecewise approximations of the book surface:

1. 2D Piecewise Polynomial Model Fitting: Represent the 2D cross section shape by m quadratic polynomials. The y axis is partitioned into m uniform intervals and the polynomial at the p -th interval is represented as follows:

$$Q_p(y) = \frac{z'_p - z'_{p-1}}{2(y_p^\Delta - y_{p-1}^\Delta)}(y - y_{p-1}^\Delta)^2 + z'_{p-1}(y - y_{p-1}^\Delta) + z_{p-1}, \quad (22)$$

where y_p^Δ ($p = 0, 1, \dots, m$) denotes the end point of a uniform interval of Δ pixels ($y_p^\Delta = y_{\Delta \times p}$), $z_p = z(y_p^\Delta)$, $z'_p = 2(z_p - z_{p-1})/(y_p^\Delta - y_{p-1}^\Delta) - z'_{p-1}$ and $z_0 = z'_0 = 0$ (just on the scanning plane). By using this model, the number of parameters to describe the cross section shape is reduced to m .

2. 3D Tessellation of the Book Surface: Approximate the 3D book surface by piecewise planar rectangles with constant albedos. By using this approximation, computation time of $I_{inter}(x_i, y_j)$ can be reduced.

5.2 Shape Recovering Algorithm

We use the following iterative algorithm to recover the cross section shape of the book surface:

step 1 Estimate the initial shape by using the optical model ignoring $I_{inter}(x_i, y_j)$ in equation (15). In this estimation, the optimal number of intervals m is also calculated based on the MDL criterion[7].

step 2 Recover the albedo distribution by using the initial shape and the observed image $P^*(x_i, y_j)$.

step 3 Calculate $I_{inter}(x_i, y_j)$ by using the tessellated book surface.

step 4 Calculate depth z_p s based on the $I_{inter}(x_i, y_j)$ obtained at step 3 and $P^*(x_i, y_j)$.

step 5 Recover the albedo distribution by using the 3D shape estimated at step 4, the $I_{inter}(x_i, y_j)$ obtained at step 3 and $P^*(x_i, y_j)$.

step 6 If all z_p s converge, then the algorithm is terminated. Otherwise repeat from step 3.

In computing z_p s in steps 1 and 4, we use the observed image intensity $P_w^*(y_j)$ at unprinted white background. $P_w^*(y_j)$ can be obtained from the observed image $P^*(x_i, y_j)$ as follows:

$$P_w^*(y_j) = \max_{x_i} P^*(x_i, y_j). \quad (23)$$

The optical model at the white background with the constant albedo ρ_w is represented as follows:

$$P_w(y_j) = \alpha \cdot \rho_w \cdot (I_{dir}(x(y_j), y_j) + I_{inter}(x(y_j), y_j)) + \beta, \quad (24)$$

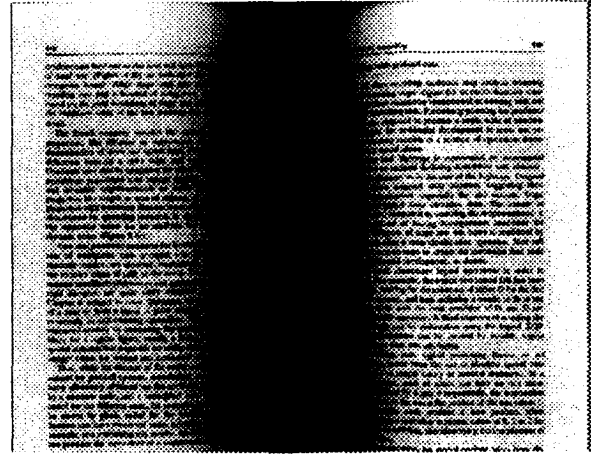


Figure 4: Observed image

where $x(y_j)$ denotes the location of the white background at y_j and we assume that ρ_w is given.

The computation of z_p s is realized by method 1 followed by method 2.

method 1 Calculate z_p sequentially by minimizing the function G in each interval:

$$G(p, z_p) = \sum_{y_j=y_{p-1}^\Delta}^{y_p^\Delta} \{P_w^*(y_j) - P_w(y_j)\}^2. \quad (25)$$

method 2 Calculate all z_p s simultaneously by minimizing the function H . In this method, the results of method 1 are used as the initial estimates of z_p s.

$$H(z_1, \dots, z_m) = \sum_{p=1}^m G(p, z_p). \quad (26)$$

6 Experiments

First, we show the experimental results of the shape estimation and the image restoration of a real book surface. Figure 4 shows an image of a book surface taken by the scanner. Figure 6 shows the estimated cross section shapes. The thin line denotes the initial estimation and the bold line the final result. Figure 5 shows the image restored by using the estimated shape. The restored image is generated by rearranging the estimated albedos. For the fine image restoration, we used the following methods: 1. enhance the contrast between the albedos at printed and unprinted areas, 2. use the cubic convolution for interpolating the albedos, 3. remove the shading along the x -axis caused by the limited length of the light source. It is confirmed that the readability of the book surface is drastically improved by the image restoration, and hence, the shape is accurately estimated enough for the image restoration.

Next, we show the experimental results using an artificial 3D model with the known shape to demonstrate

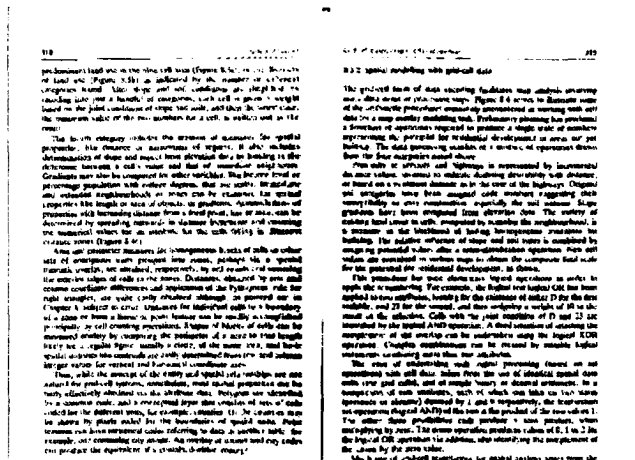


Figure 5: Restored image

Table 1: Effectiveness of the piecewise polynomial model fitting

	number of parameters	time ratio	(real [min.])	error [mm]
piecewise	15	1	(1.18)	0.94
pointwise	480	233	(276.17)	1.28

Table 2: Effectiveness of the tessellated book surface

n	number of rectangles	time		error [mm]
		interreflections ratio (real [sec.])	reconstruction ratio (real [min.])	
1	2	0.0026 (0.07)	2.9 (1.3)	22.04
5	50	0.028 (0.76)	3.7 (1.7)	3.46
10	200	0.11 (2.90)	3.1 (1.5)	2.19
20	800	0.43 (11.8)	4.4 (2.1)	2.03
40	3200	1.67 (46.2)	11.4 (5.4)	2.16
pointwise	628145	100.0 (2735.5)	100.0 (47.1)	2.35

the effectiveness and accuracy of the proposed algorithm. Table 1 shows the computation time (SPARC station 10) to recover the shape and the mean error of the estimated shape by the piecewise polynomial model fitting and the pointwise estimation method⁴. This result demonstrates that the piecewise shape approximation drastically reduces the computation time. Moreover, the accuracy of the estimation is improved, because the piecewise approximation is stable against noise. Table 2 shows the computation times and the mean errors by $n \times n$ tessellation of the book surface. We can observe that the tessellation with adequate number of rectangles, such as $n = 20$, greatly reduces the computation time while keeping the accuracy.

7 Conclusions

In this paper, we discussed the real world problem to recover the 3D shape of the book surface from a scanner image. It is shown that this problem can be

⁴In this experiment, half of the book shape ($y > 0$) is recovered from the image without interreflections.

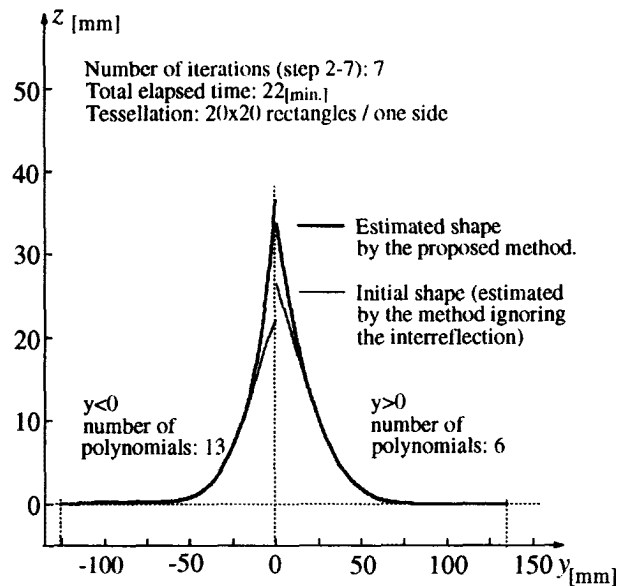


Figure 6: Estimated shapes

solved by an iterative non-linear optimization problem to estimate the interdependent parameters: shape, depth and albedo. To improve the efficiency and stability, we employed the piecewise approximations of the shape and the albedo distribution. Some experimental results demonstrated that the proposed algorithm can recover the 3D shape accurately and efficiently.

Future works includes problems under the following conditions: 1. the center line separating book pages is not aligned parallel to the x -axis, 2. the reflectance property of the book surface is not given a priori.

References

- [1] B.K.P.Horn: "Obtaining shape from shading information", The Psychology of Computer Vision, P.H.Winston, ed., McGraw-Hill Book Co., New York, pp.115-155, 1975
- [2] R.J.Woodham: "Photometric method for determining surface orientation from multiple images", Opt. Eng., 19, 1, pp. 139-144, Jan./Feb. 1981
- [3] K.Ikeuchi: "Determining 3D Shape from Shading Information Based on the Reflectance Map Technique", Trans. IECE Japan, Part D, J65-D, 7, pp.842-849, 1982-07
- [4] M.Asada: "Cylindrical shape from contour and shading without knowledge of lighting conditions or surface albedo", Proc. of ICCV, pp.412-416, 1987
- [5] S.K.Nayar, K.Ikeuchi, and T.Kanade: "Shape from Interreflections", ICCV, pp.2-11, 1990
- [6] H.D.Ballard, C.M.Brown: "Computer Vision", Prentice Hall, Inc., Englewood Cliffs, New Jersey, pp.93-102, 1982
- [7] J.Rissanen: "Modeling By Shortest Data Description", Automatica, Vol.14, pp.465-471, 1978